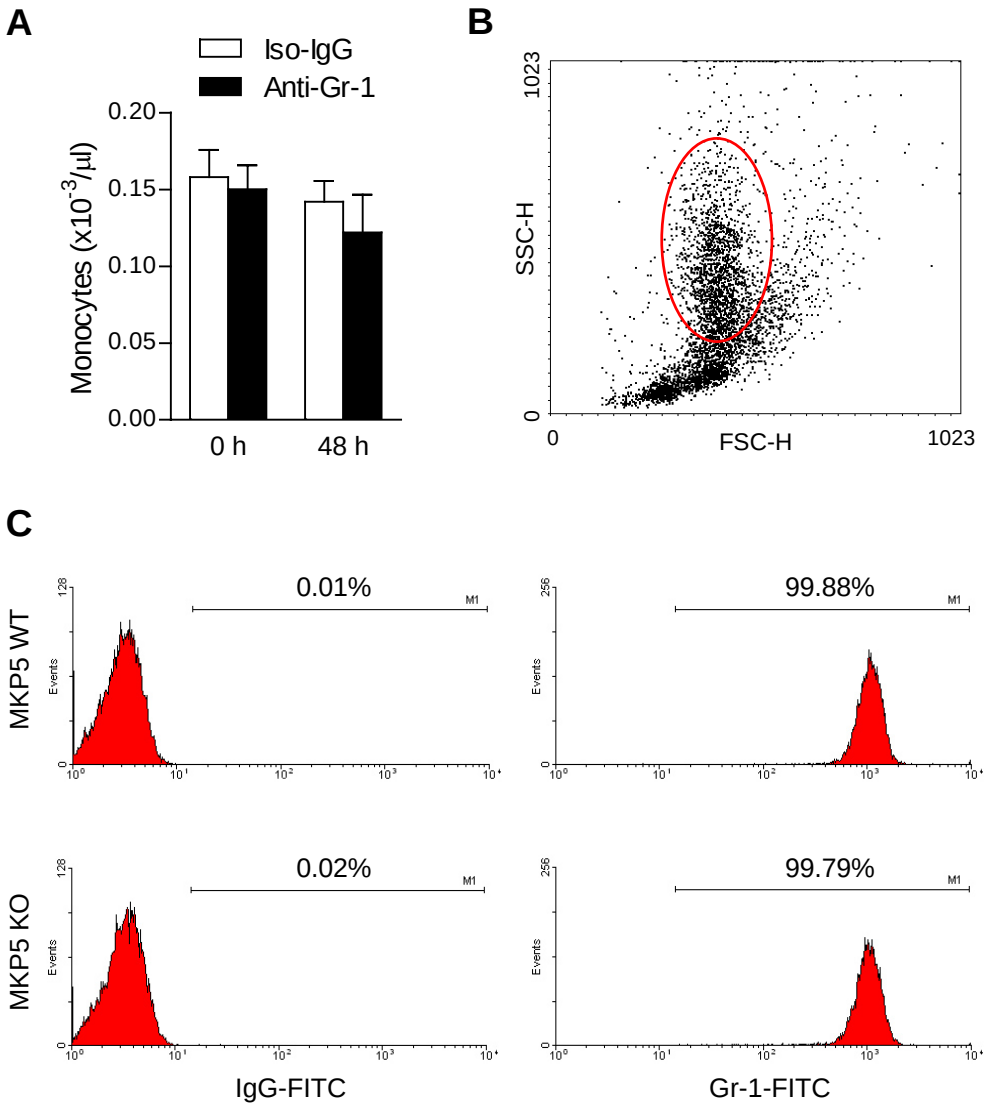

Figure S1. Effects of anti-Gr-1 antibody on peripheral blood monocytes count and purification of neutrophils. (**A**) Peripheral blood monocytes count in *Mkp5*$^{-/-}$ mice, determined at 0 h and 48 h after *i.p.* injection of anti-Gr-1 anitbody (RB6-8C5, filled bars) and compared with the count in mice receiving isotype-matched IgG (Iso-IgG, open bars). Data shown are mean ± SEM based on 3 independent experiments. No statistically significant difference was detected between the samples ($p > 0.05$). (**B**) WT and *Mkp5*$^{-/-}$ neutrophils prepared by density gradient centrifugation were subjected to side scatter-activated sorting. The sorted cells (circled in B) were then stained with an FITC-labeled 1A8 antibody (Ly-6G specific) and analyzed. The proportions of Gr-1^{+} and Gr-1^{-} cells within the sorted cells are shown in (**C**). The purity of Gr-1^{+} cells reached 99.88% in WT and 99.79% in *Mkp5*$^{-/-}$ cell populations. Eosin positive cells are less than 1%.

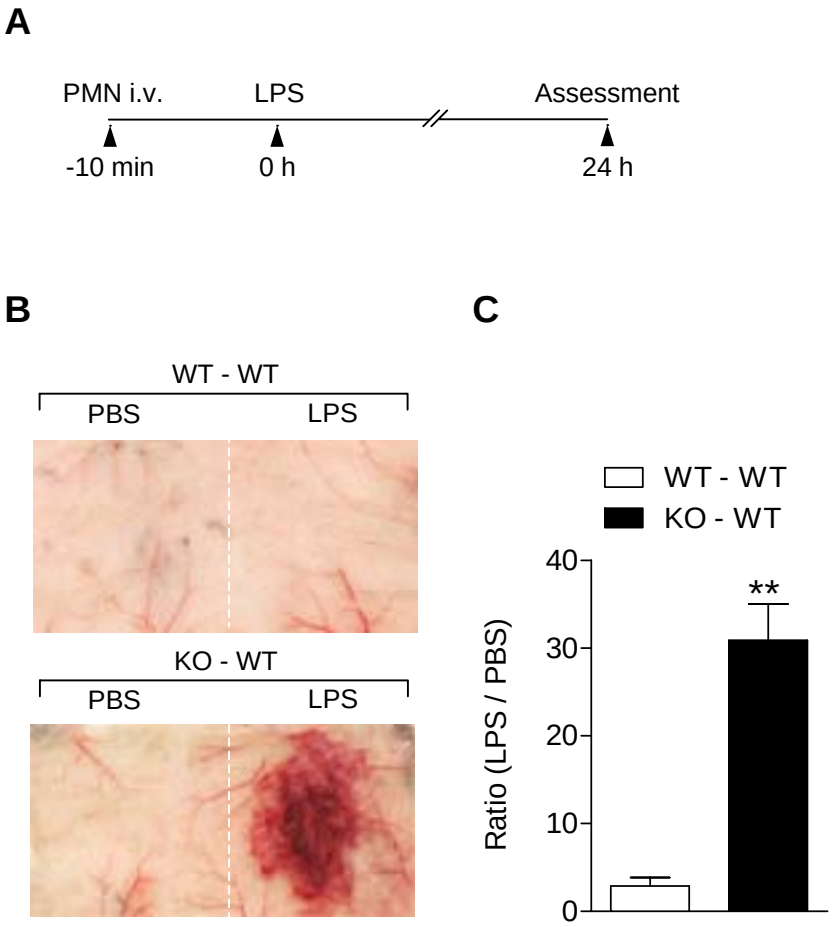

Figure S2. Adoptive transfer of highly purified *Mkp5*$^{-/-}$ neutrophils leads to exacerbated LSR in WT recipients. WT mice were intravenously injected with purified WT and *Mkp5*$^{-/-}$ (KO) neutrophils (2×10^6, after side scatter-activated sorting) using the scheme in (**A**). After 10 min, 80 μg LPS was administered *s.c.* to dorsal skin. Macroscopic appearance of the LPS injection site was imaged at 24 h (**B**). The extent of hemorrhage was quantified by densitometry and shown in (**C**). Data were based on 3 independent experiments. **, $p < 0.01$.

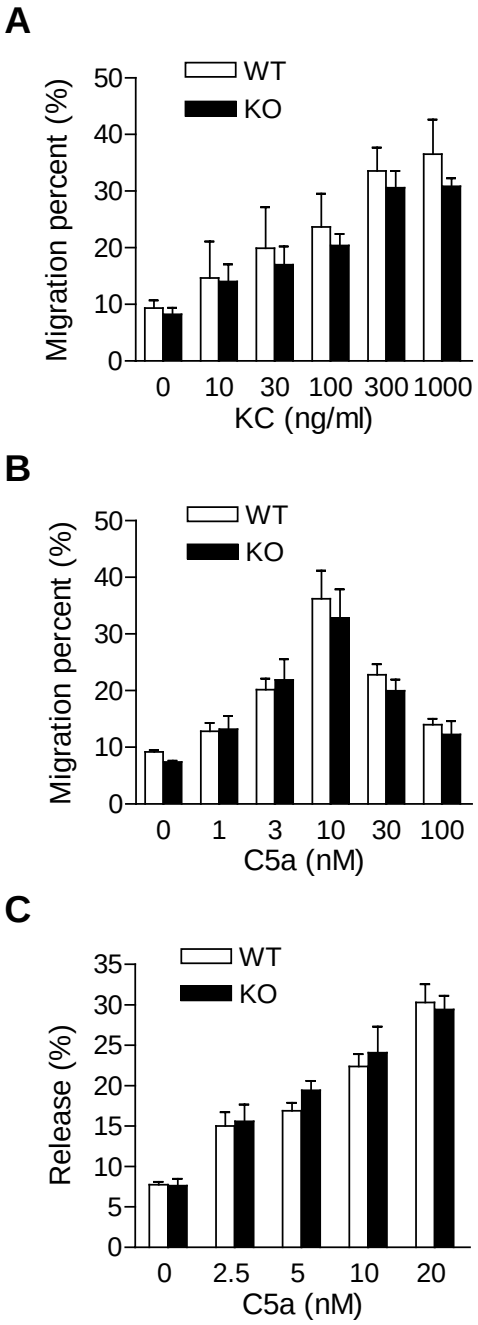

Figure S3. Absence of difference in chemotaxis and degranulation between WT and *Mkp5*$^{-/-}$ neutrophils. Neutrophil chemotaxis in response to KC (**A**) and C5a (**B**) was determined as described in *Materials and Methods*. No significant difference was found between the WT and *Mkp5*$^{-/-}$ (KO) neutrophils ($p > 0.05$). (**C**) C5a induced dose-dependent release of β-glucuronidase from neutrophils. Again, no significant difference was observed between the WT and *Mkp5*$^{-/-}$ neutrophils ($p > 0.05$).

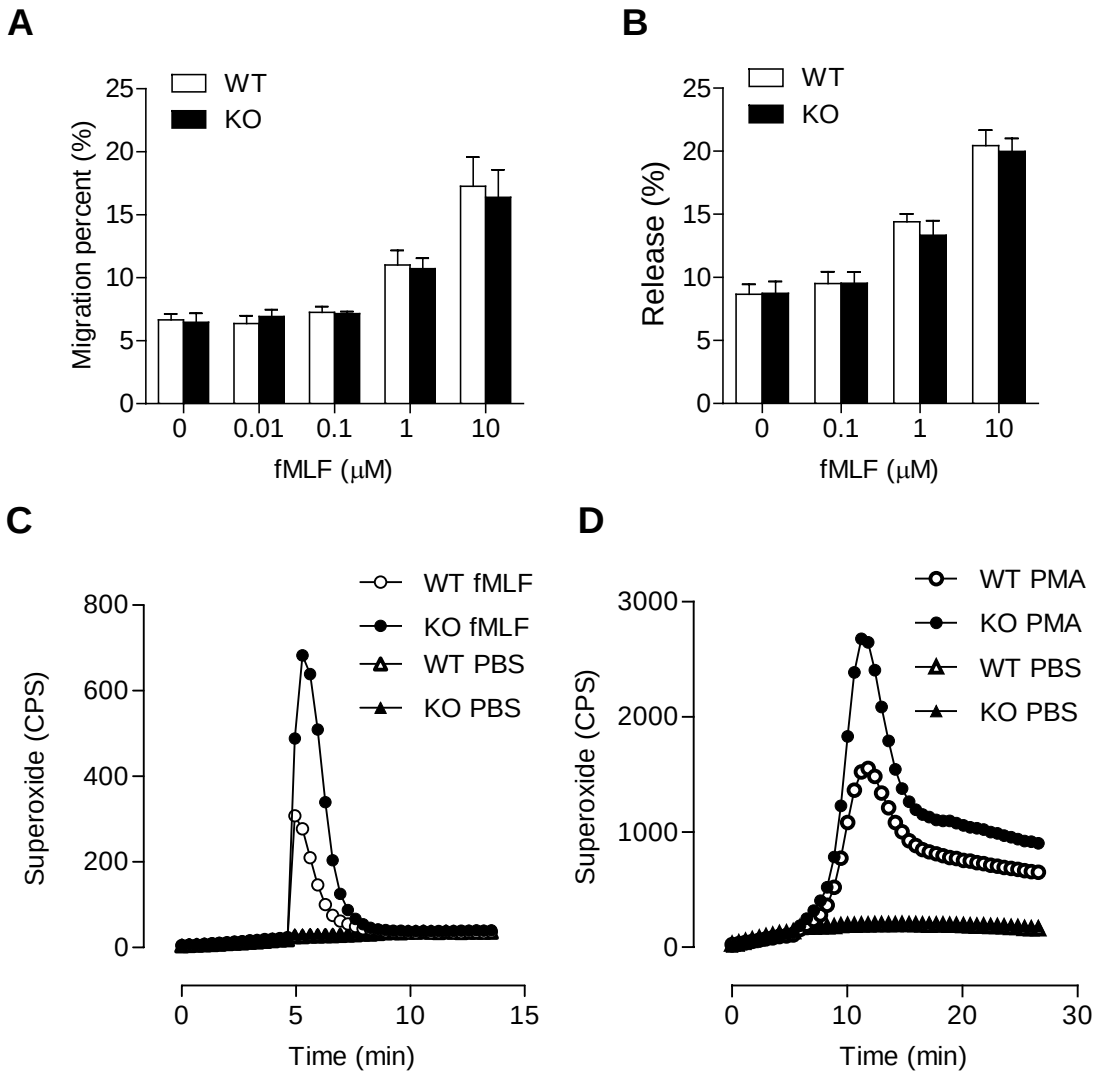

Figure S4. Effect of MKP5 deficiency on fMLF- and PMA-induced neutrophil activation. (**A**) Chemotaxis of WT and *Mkp5*$^{-/-}$ (KO) neutrophils towards fMLF was determined in transwell assays. (**B**) fMLF induced dose-dependent release of β-glucuronidase from both WT and *Mkp5*$^{-/-}$ neutrophils. Data shown in **A** and **B** are mean ± SEM from 3 independent measurements, and no statistically significant difference was see ($p > 0.05$ between all samples). (**C** and **D**) Reduction in superoxide production in *Mkp5*$^{-/-}$ neutrophils stimulated with fMLF (**C**, 10 μM) or PMA (**D**, 200 ng/ml). Representative tracings from at least 3 repeating experiments are shown.

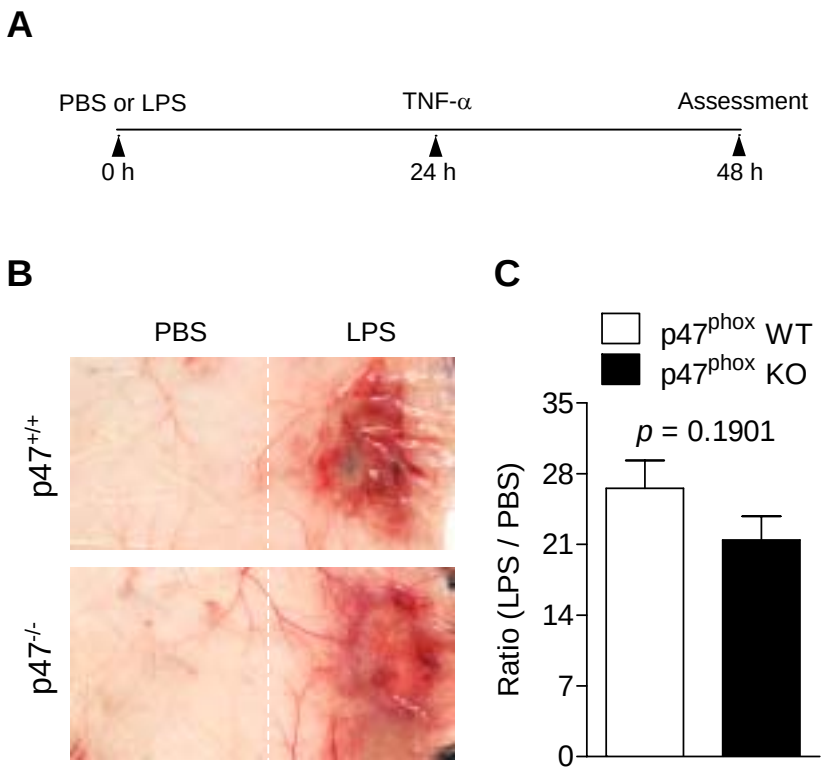

Figure S5. Comparison of p47$^{phox+/+}$ and p47$^{phox-/-}$ mice in the classic LSR. The classic LSR was induced as described in the legend for Figure 1 and shown schematically in (**A**), using p47^{phox} WT and KO mice. The mice were sacrificed 24 h after the second injection, and the skin tissues were examined macroscopically (**B**). The extent of hemorrhage was quantified by densitometry analysis of skin samples receiving LPS injection, and compared to the contralateral side which received PBS injection. Data shown are mean ± SEM (n = 3). The difference was statistically insignificant (p = 0.1901).

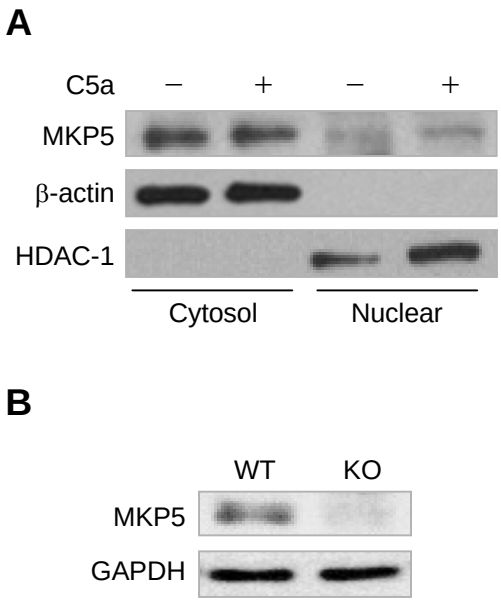

Figure S6. MKP5 expression and subcellular localization in mouse neutrophils. (**A**) The cytosol and nuclear fractions of resting or C5a-stimulated (100 nM, 5 min) mouse bone marrow neutrophils were separated on SDS-PAGE as described in *Materials and Methods.* The presence of MKP5 in the cytosol and nuclear fractions was detected using an anti-MKP5 antibody for Western blotting. HDAC-1 and β-actin were used as the nuclear and cytosol markers, respectively. (**B**), Western blotting comparing MKP5 expression in WT and *Mkp5* $^{-/-}$ bone marrow neutrophils.

Supplementary Materials and Methods (Qian et al.)

Purification of mouse neutrophils for adoptive transfer

Mouse neutrophils were prepared from bone marrow by density gradient centrifugation, and then subjected to side scatter-activated sorting on a MoFlo cell sorter (Becton Dickinson) for granulocytes (circled in Figure S1). The sorted cells were stained with a FITC-anti-Gr-1 anitbody (clone 1A8, Ly-6G specific; BD Pharmingen) and analyzed. Fluorescence histograms were generated using the WinMDI 2.9 software.

Chemotaxis and degranulation assays

Chemotaxis assays were performed using Transwell inserts with 5 μm pores (Corning). Each well contained 2×10^6 neutrophils. Checkerboard analysis was conducted by addition of various concentrations of the chemoattractants (KC, C5a and fMLF) to the inserts to determine the effect of chemokinesis on directional cell migration. After 30 min at 37°C, migrated neutrophils were collected and counted by flow cytometry. Neutrophil release of β-glucuronidase was detected as described previously (Nanamori et al., 2007).

Classic local Shwartzman reaction

Mice (8-10-wk old) were anesthetized with an *i.p.* injection of ketamine (100 mg/kg) and xylazine (5 mg/kg) in sterile PBS. The right dorsal skin was injected with 80 μg of LPS in 80 μl PBS. After 24 h, 0.2 μg of TNF-α (R&D Systems) in 20 μl PBS was injected to the same site. The left dorsal skin was injected with equal volume of PBS as control. The mice were sacrificed at 48 h and dorsal skin was excised for photo documentation.

Detection of MKP5 in neutrophils

Mouse neutrophils (1×10^7 cells/sample) from WT and *Mkp5*$^{-/-}$ bone marrow were lysed in buffer containing 20 mM Tris-HCl, pH 7.6, 150 mM NaCl, 5 mM EDTA, 1 mM Na-orthovanadate, 20 μM 4-(2-aminoethyl)-benzenesulfonyl fluoride, 1% triton X-100, 5 μg/ml leupeptin, and 1:100 of Calbiochem Protease Inhibitor Cocktail Set 1. The cell lysate was separated on SDS-PAGE and analyzed with Western blotting, using an anti-MKP5 antibody (Abcam). To determine MKP5 subcelluar localization, WT neutrophils (1×10^7) were stimulated with 100 nM C5a or buffer control for 5 min at 37°C. The stimulated cells were collected and incubated with 400 μl NEB-A buffer (10 mM HEPES, pH 7.9, 0.5% NP-40, 10 mM KCl, 0.1 mM EDTA, 0.1 mM EGTA, 1 mM DTT, 1 mM PMSF and 1:100 of Calbiochem Protease Inhibitor Cocktail Set 1) for 10 min on ice. After centrifugation at 1,500 g for 5 min, the supernatant was collected as the cytosol fraction. The cell pellet was washed with cold NEB-A buffer for five times, and then incubated with 100 μl NEB-B buffer (20 mM HEPES, pH 7.9, 0.4 M NaCl, 1 mM EDTA, 1 mM EGTA, 1 mM PMSF and Calbiochem Protease Inhibitor

Cocktail Set 1) for 30 min. After centrifugation at 10,000 g for 5 min, the supernatant was collected as the nuclear fraction. The subcellular fractions were separated on SDS-PAGE and analyzed with Western blotting. The nuclear marker HDAC-1 and the cytosolic marker β-actin were detected by an anti-HDAC-1 antibody (Millipore) and an anti-β-actin antibody (Sigma), respectively.

Supplementary Reference

Nanamori, M., Chen, J., Du, X. and Ye, R.D. (2007) Regulation of leukocyte degranulation by cGMP-dependent protein kinase and phosphoinositide 3-kinase: potential roles in phosphorylation of target membrane SNARE complex proteins in rat mast cells. *J Immunol*, 178, 416-427.